The Wind Stress Patterns over the Indian Ocean During the Summer Monsoon of 1979

DONALD P. WYLIE AND BARRY B. HINTON

Space Science and Engineering Center, University of Wisconsin-Madison, 53706

(Manuscript received 27 March 1981, in final form 9 November 1981)

ABSTRACT

A detailed analysis of the wind stress patterns over the Indian Ocean was made from 1 May to 31 July 1979. A combination of cloud motion and ship data obtained once per day was used to diagnose the surface-wind patterns to a degree of detail not possible in the past for an individual season. These data show the monsoon development and the fluctuations of the Somali Jet and the Southern Hemispheric tradewinds. Wind stress patterns produced by two traveling tropical storms are discussed. These combined to exert an unusually high westerly wind stress on the equator before the monsoon developed.

1. Introduction

Detailed data on the wind stress, a primary forcing mechanism, are needed to quantitatively understand ocean circulations. During the World Weather Watch of FGGE (First GARP Global Experiment) and the summer MONEX (Monsoon Experiment) program (Fein and Kuettner, 1980) a unique set of wind observations was obtained from tracking cloud motions (Young *et al.*, 1980) over the Indian Ocean. A logical use of these data would be to estimate the wind stress on the ocean. The intent of this paper is to summarize these stress patterns.

Ship observations and scientific expeditions have provided a sparse collection of data from which general wind patterns can be inferred but at a density too low for detailed studies of the patterns over whole ocean basins. Perhaps the best stress patterns over the Indian Ocean are the climatologies compiled by Hastenrath and Lamb (1979), Hellerman (1967), and Bruce (1978). These were derived by compositing many years (~20–60) of merchant ship observations. While these climatologies depict the general wind patterns, they cannot give quantitative details on the events of one season in one year.

The FGGE and MONEX investigations provided large volumes of atmospheric and oceanic data over the Indian Ocean during the summer monsoon of 1979. In this paper we will focus on the development of the summer monsoon. We made wind stress analyses on observations obtained once each day from 1 May to 31 July 1979. We hope our quantitative wind stress data set will benefit diagnostic and modeling studies of the Indian Ocean.

2. The data used

We have combined data from two complimentary sources: The cloud-motion observations and the merchant-ship reports. This combination alleviates certain problems caused by the weaknesses in each type of data and provides a composite analysis that uses the strength of each type. For example, cloud motions provided good coverage over most of the Indian Ocean except the northern Arabian Sea and the Bay of Bengal. But at the beginning of the study period, the first two weeks of May, there were few clouds in these areas so we could not obtain a good analysis of the wind fields during that time from cloud motions alone.

Fortunately, the merchant-ship routes crossed the areas where the cloud-motion coverage was poor. Thus, a combination of data types defined the wind patterns better than either taken alone. The methods used for compositing these data and correcting the cloud motions for wind shear in the atmospheric boundary layer are described below.

a. The cloud-motion data

Cloud motions were tracked on the images made by the geostationary satellite (a standard United States GOES model) positioned over the Indian Ocean at ~57° east longitude. Data were obtained by operators at the Madison and Milwaukee campuses of the University of Wisconsin, who manually selected cloud tracers using the Man-computer Interactive Data Analysis System (McIDAS).

A series of three satellite images was used. These were taken at 0.5 h intervals in the time period from 0830 to 1100 GMT. This period was during the daytime when clouds could be tracked in the visible satellite images. Normally the 0830, 0900 and 0930 GMT images were used. However, if one of these was of low quality or absent a series as late as 1000, 1030 and 1100 was used. A second cloud-motion analysis was made 12 h later using infrared images;

0022-3670/82/020186-14$07.50

however, a malfunction in the sensor caused the loss of the infrared images during ~60% of the days studied. Because the infrared analysis was incomplete, we used only the cloud-motion analysis obtained from the visible data.

For each cloud tracer tracked, two motion vectors were calculated using the three pictures in the sequence. The cloud displacements were derived objectively from correlation algorithms applied to the digital satellite data. A first guess of the cloud's movement provided by the operator speeded the calculation by allowing smaller areas to be used in the correlation. Quality control editing was automatically applied in the correlation algorithm. In addition, the two vectors derived for each cloud were compared for consistency.

Additional quality checks were carried out by the target selection operator who inspected each calculation with the satellite image sequence immediately after it was made. Both vectors in each pair that passed all the quality controls were averaged to form one vector for each cloud tracer. More details on the Wisconsin wind analysis system are given in Mosher (1979).

From 1 May to 31 July 1979 ~800 motion vectors per day were extracted from the low-level cloud fields. The area cover by the cloud tracking system was from 40 to 110°E longitude and 40°N to 40°S latitude. These vectors were objectively analyzed to a 2° latitude × 2° longitude grid inside this area using the method of Endlich and Mancuso (1968). The resulting grids were presented in an atlas by Young *et al.* (1980).

The analysis applies the weighting function given by

$$w = 4./(4. + R^2) \qquad (1)$$

to the vectors closest to each grid point location. In (1) R represents the distance from the vector location to the grid point in degrees of arc on the earth's surface. This function approximates a Gaussian low pass filter. Note that a value ≤ 0.5 would be assigned any vector more than 2° from the grid point. No vectors more than 6° from a grid point were used. Where less than two vectors were found inside this area, the grid point was not filled.

In the present paper we have restricted the study area to the central Indian Ocean from the East African coast to 96°E longitude and from the Southern Asian coast to 32°S latitude. The Red Sea and the Persian Gulf also were excluded.

b. The ship data

The marine deck compiled by the FGGE Level IIb Mobile Ship Data Center in Hamburg, F.R.G. was the source of ship data for this analysis. An average of 177 observations per day were found in the Indian Ocean. For the daily surface wind analysis all ship reports taken from 0000 to 2100 GMT on each day were used. The satellite analysis was made in the middle of this time period.

To weed out the bad ship reports an automatic editing function was applied to the ship data on a daily basis. Each report was compared to the average of all other ships within 5° latitude or longitude. If the report differed by >45° in direction or 5 m s^{-1} in speed from the vector average of the other ships the report was eliminated. A minimum of two external reports were required to define the average wind around each report examined. If less than two neighboring reports were found, the report was deleted. This procedure eliminated an average of 13% of the ship reports on each day studied.

3. The method of data combination

In order to use the cloud-motion data as estimates of the surface winds, corrections had to be applied for the wind shear in the atmospheric boundary layer below the clouds. These corrections were empirically derived by comparing co-located ship and cloud observations (see Wylie and Hinton, 1981). Each ship observation that passed the editing procedure was compared to the cloud motion analysis at the nearest grid point. A total of 4293 cloud–ship comparison pairs were found for the three month period. From these we derived statistical relationships between the cloud motions and ship reported winds.

A linear relationship was used to account for the sub-cloud shear of the wind speed, i.e.,

$$S_{sfc} = 0.72S_{cld} + 1.2. \qquad (2)$$

This relationship fit the cloud-ship comparisons with a rms scatter of 2.6 m s^{-1}.

The cloud–ship directional relationships were more complicated. They varied with latitude, direction of the basic flow, and wind speed. The corrections for the cloud direction were derived in six geographical areas that were mainly divided by latitude. Within each area the correction depended on which quadrants the winds were blowing from. However, in some areas the wind directions were mostly in one or two quadrants and meaningful statistics for other quadrants could not be obtained. Where this situation occurred, the directional corrections were assumed (see Table 1).

It follows that the assumed values apply to cases which occur infrequently (e.g., southern trades from the west). Hence they should affect the 10-day, or longer, mean fields only slightly. Where an entry was available for speeds <10 m s^{-1}, but not greater, a value based on the lower speed range was used. In some cases this was modified by the trend of the few observations available.

The directional corrections applied ranged from

TABLE 1. Directional corrections applied to the cloud motion analyses to account for the wind directional shear below the cloud level. The corrections were developed from the statistics shown in Wylie and Hinton (1981).

Location	Cloud speed ≤ 10 m s^{-1}				Cloud speed > 10 m s^{-1}			
	N	E	S	W	N	E	S	W
Arabian Sea (coast–9°N)	+47°	+33°	−5°	+21°	+50°*	+20°*	+21°*	+12°
Bay of Bengal (coast–9°N)	+25°*	+20°*	12°*	+33°	+20°*	+15°*	0*	+10°
Somali coast (9°N–5°S, Coast–65°E)	+25°*	+1°	−8°	+11°	+25°*	−11°*	−2°	+3°
Equatorial latitudes (9°N–5°S, 65–96°E)	+24°	−13°	−8°	+14°	+20°*	−10°*	−7°*	+10°
Southern trades (5–21°S)	−20°*	−18°	−5°	−19°*	−20°*	−14°	−5°	−19°*
Southern midlatitudes (21–32°S)	−39°	−12°	+2°	+13°	−41°*	−10°	+3°	−3°

* Because of the small sample sizes these entries in the table are less certain, and in a few cases have been chosen arbitrarily as explained in the text, as in the similar table in Wylie and Hinton (1981).

+47° in the Northern Hemisphere to −39° in the Southern Hemisphere. For the higher wind speeds, cloud motions >10 m s^{-1}, the directional corrections tended to be smaller ranging from −12° in the Arabian Sea to +14° in the Southern Hemisphere trades if the quadrants containing very few observations were not considered. In general, the cloud–ship directional scatter also was lower under the higher wind conditions (see Wylie and Hinton, 1981). Thus, we feel our analyses are more accurate in the areas of high winds than areas of light winds.

After correcting the cloud motion grids for boundary-layer shear, the ship data were added. The ship reports were analyzed at grid points using the same weighting function as the cloud motion grids (1). The cloud-motion value at each grid point was added with a relative weight of 0.5. Thus, for grid points where only one ship report at 2° distance were found, ship reports and the cloud motion analysis were weighted equally. For grid points where one or more ship reports closer than 2° distance were found, the ship reports dominated the resultant analysis. Where no ship reports within 6° of latitude or longitude were available, the cloud motion analysis (corrected for shear) was used exclusively.

The decision to mix data sets in this way was somewhat arbitrary. It is conventional to weight data so that each set of measurements contributes equally to the expected variance of the estimate from the truth. This means that the relative weights would be inversely proportional to the variance. In another paper (Wylie and Hinton, 1981) we showed that the wind analysis correlated with a nearby ship (<1° from the grid point) to about the same degree as two closely spaced ships. Although there is no "truth" available to ascertain the actual variance of each data set, this approximate equality of correlation coefficients suggests that ship data and the cloud analysis should be mixed with roughly equal weight out to 1° separation. We chose to tip the balance slightly in favor of the ship observations to expand the areas in which the analysis results from data of both kinds. A weighting scheme based on numbers of observations of each type would produce an analysis nearly free of the direct influence of the *in situ* ship data almost everywhere.

The ship reports were concentrated along the lines of the main merchant routes. Most of the reports were found along a line from Malaysia to Sri Lanka to the Red Sea across the Northern Indian Ocean. Several reports were obtained each day north of this line in the Arabian Sea. A second route along the East African Coast also contained several reports each day. A minor trade route from Malaysia to South Africa through the center of the Indian Ocean contained reports on some of the days analyzed. Outside of these areas few ship data were found. Even with the extra weight given ships, wind analyses were primarily from the cloud motion data. More details on the locations of the ship data can be found in Wylie and Hinton (1981).

The daily surface-wind analyses produced from the cloud–ship combination were converted to surface stress (τ) estimates using the bulk aerodynamic formula

$$\tau = \rho C_d |\mathbf{U}| \mathbf{U}, \tag{3}$$

where $\mathbf{U}$ is the wind and ρ is the air density which was assumed to vary with latitude from 1.16 kg m^{-3} at 20°N to 1.21 kg m^{-3} at 30°S. A drag coefficient, given by (4), that was a linear function of wind speed was used following the recommendation of Wu (1980):

$$C_d = (0.8 + 0.065|\mathbf{U}|)10^{-3}. \tag{4}$$

4. Monthly mean patterns

a. May 1979

During May the easterly tradewinds from 5 to 25°S were strong throughout the month (Fig. 1).

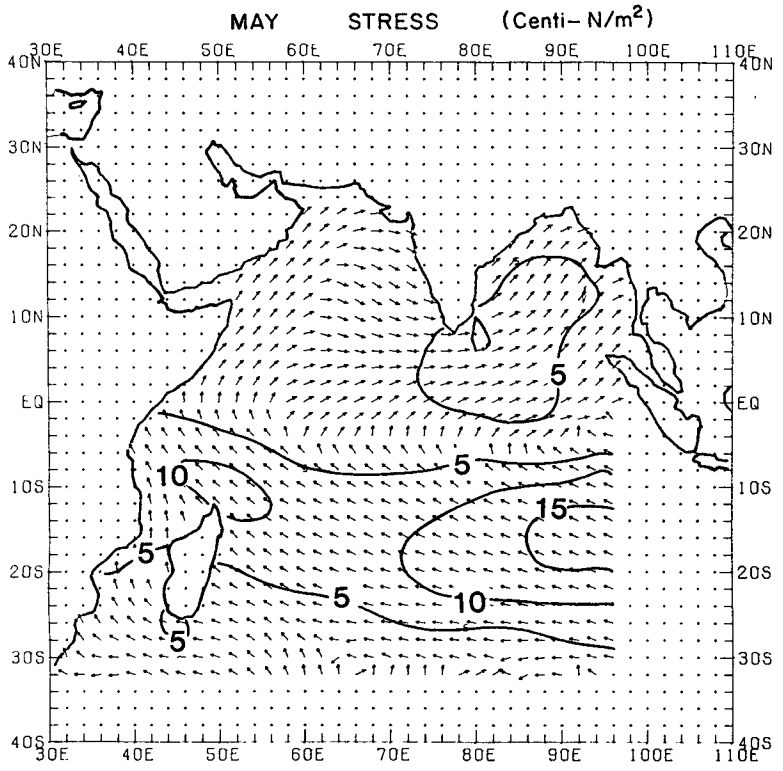

FIG. 1. Average wind stress for May 1979. The vectors indicate the directions of the surface winds at 2° grid spacings. The contours indicate magnitudes of the stress in units of 0.01 N m^{-2} (0.01 Pa), equivalent to 0.1 dyn cm^{-2}.

There were two areas of notably high winds. One was off the north coast of Madagascar and the other on the eastern side of the Indian Ocean at 15°S and 90°E. North of Madagascar the winds were consistently from the southeast while upwind on the eastern side of the study area the the winds were somewhat enhanced by a traveling vortex that appeared early in May. This vortex will be discussed further in the next section.

Arabian Sea winds were very weak throughout the month. Although the wind direction had shifted to the southwest, approximately the expected direction of the monsoon (Hastenrath and Lamb, 1979), there was little stress on the sea. Similarly, in the Bay of Bengal the wind directions corresponded to the climatological direction for the summer season but with very low speeds. This is in accordance with Hastenrath and Lamb (1979) who show a pronounced shift in direction between the chart for April and the May chart, which resembles the June–August directional pattern in the Arabian Sea as well as the Bay of Bengal. Convective disturbances present in the latter area caused variability in the wind directions resulting in a weak mean stress.

In the Arabian Sea, however, the climatology indicated moderately strong (~7 m s^{-1} maximum) southwest winds while our analysis found only ~5 m s^{-1} during the month. This could be a reflection of the later than normal onset of the monsoon during the 1979 season (Fein and Kuettner, 1980). We found the May 1979 trades to be nearly the same strength and direction as the climatological field of Hastenrath and Lamb (1979).

b. June 1979

During June the monsoon attained nearly full strength (Fig. 2). The southwesterly winds in the Arabian Sea developed into the very strong Somali Jet with cloud motions often in excess of 25 m s^{-1}. Our analysis estimated the surface stress to be in excess of 0.3 N m^{-2} (3 dyne cm^{-2}).

The Somali Jet appeared more vividly in our stress analyses than our surface wind analyses. When the quadratic aerodynamic stress parameterization (3) was combined with a drag coefficient (4) the stress increased with the cube of the speed for speeds much above 10 m s^{-1}. Hence, the areas of strong winds exerted a larger force on the ocean than was apparent from the wind analyses.

The stress exerted by the trade winds south of the equator was also stronger in June than in May. Most of the area had an average stress $\geq$0.1 N m^{-2} ($\geq$1 dyn cm^{-2}). The June 1979 tradewinds were approx-

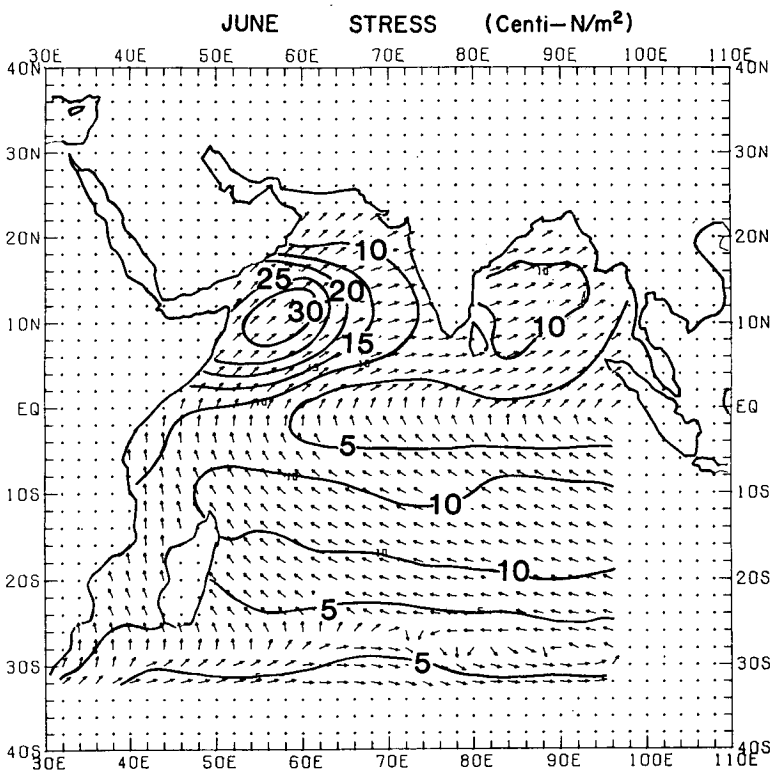

FIG. 2. Average-wind stress for June 1979.

imately the same strength as the Hastenrath and Lamb climatology. The Somali Jet was weaker than the climatology partly due to the late development of the monsoon.

c. July 1979

During July the Somali Jet was even stronger than in June. As shown in Fig. 3 the maximum stress was >0.45 N m^{-2} (4.5 dyne cm^{-2}). A clear S-shaped pattern was very similar to the climatological wind pattern shown in Hastenrath and Lamb (1979). The magnitude of our July-averaged Somali Jet also was close to the climatological average. The only area where the July 1979 analysis differed noticeably was the Southern Hemisphere trades which were slightly weaker.

5. Temporal changes in the stress patterns

To present a record of the temporal variations of the stress we have compiled a series of 10-day average-stress maps (Figs. 4–12). Each 10-day average was made from the daily calculations of the stress on the 2 × 2° grids as previously discussed.

During the first 10-day period in May two storm systems were present in the eastern Indian Ocean. A tropical storm in the Northern Hemisphere moved along a track from a position at 4°N, 92°E on 1 May toward the northwest, reaching India on 11 May at 13°N, 80°E. At the same time a companion vortex moved westward very slowly from a position at 5°S and 92°E on 1 May to a position at 6°S and 88°E on 8 May.

The northern storm system exhibited many cirrus anvils on the satellite images (see Young *et al.*, 1980; Rao, 1980) indicating that many cumulonimbus clouds were present. In contrast the southern storm had far fewer cirrus anvils.

From 8 to 17 May the cirrus clouds associated with the southern vortex disappeared but the vortex moved westward and at a faster speed. It was last diagnosed as a vortex on the wind analysis of 17 May at 4°S and 68°E.

A result of the two large vortexes positioned ~10° latitude apart in opposite hemispheres was a strong westerly wind that developed between the storms. Because the two vortexes rotated in opposite directions, their strength added at the equator. A westerly jet appeared on the wind analyses on the equator at 82°E. It reached a maximum strength of 12 m s^{-1} on 5 May. There was some variance in the diagnosis of the jet and the vortexes from day to day because of sampling problems. Obscurations of the low-cloud motions by cirrus clouds prevented detailed analyses on some of the days during this period. Thus the 10-day averaged stress of 0.15 N m^{-2} shown in Fig. 4 may have been a slight underestimate.

Outside these storm systems the wind analyses were seldom obscured. The trade winds in the Southern Hemisphere, in particular, were well diagnosed

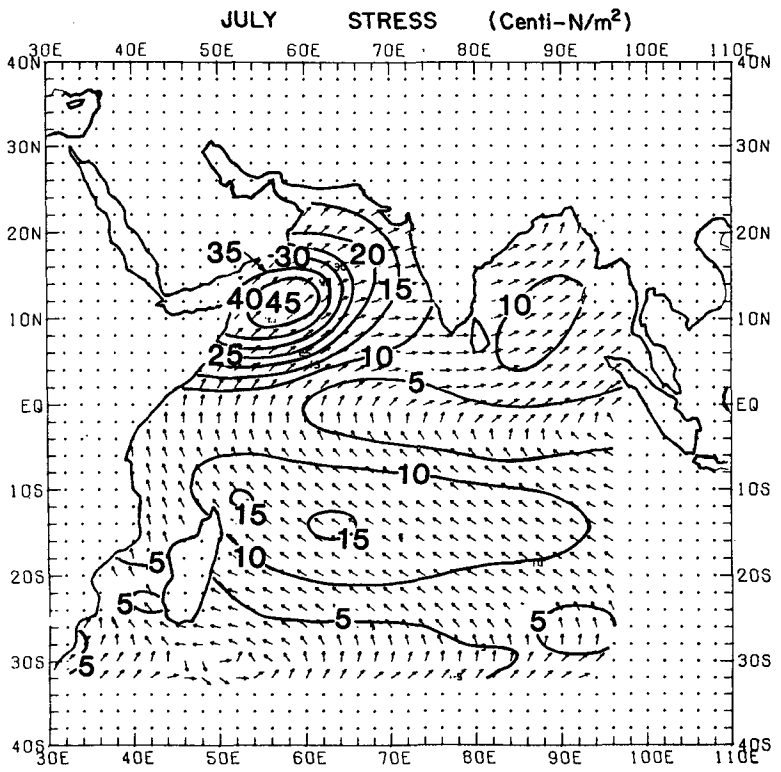

FIG. 3. Average-wind stress for July 1979.

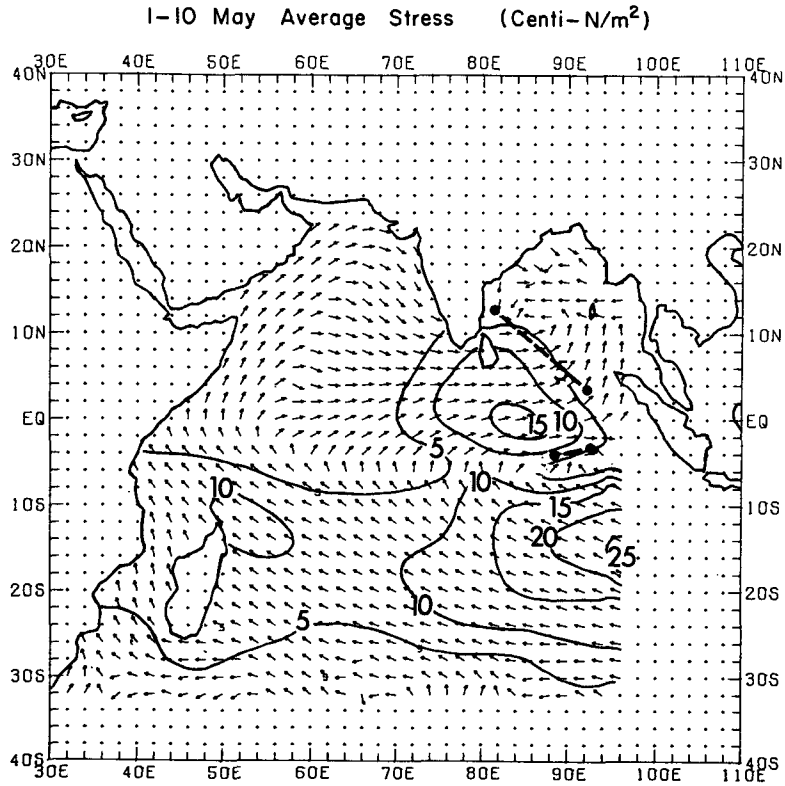

FIG. 4. Average-wind stress from 1 to 10 May 1979. The tracks of two tropical storms in both hemispheres are shown by dashed lines (see text).

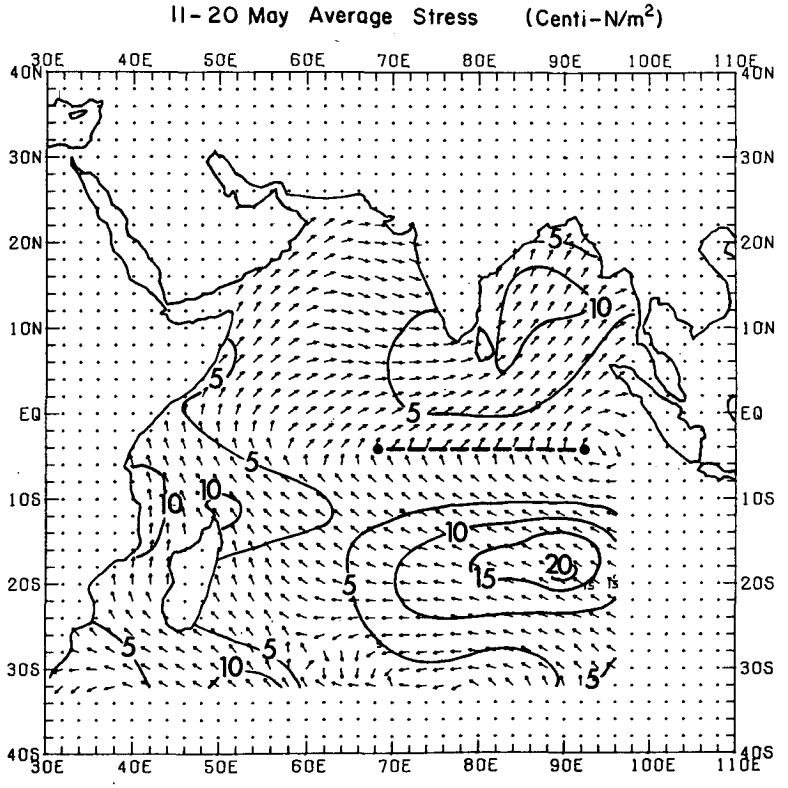

FIG. 5. Average wind stress from 11 to 20 May 1979. The track of the Southern Hemisphere vortex is indicated by the dashed line.

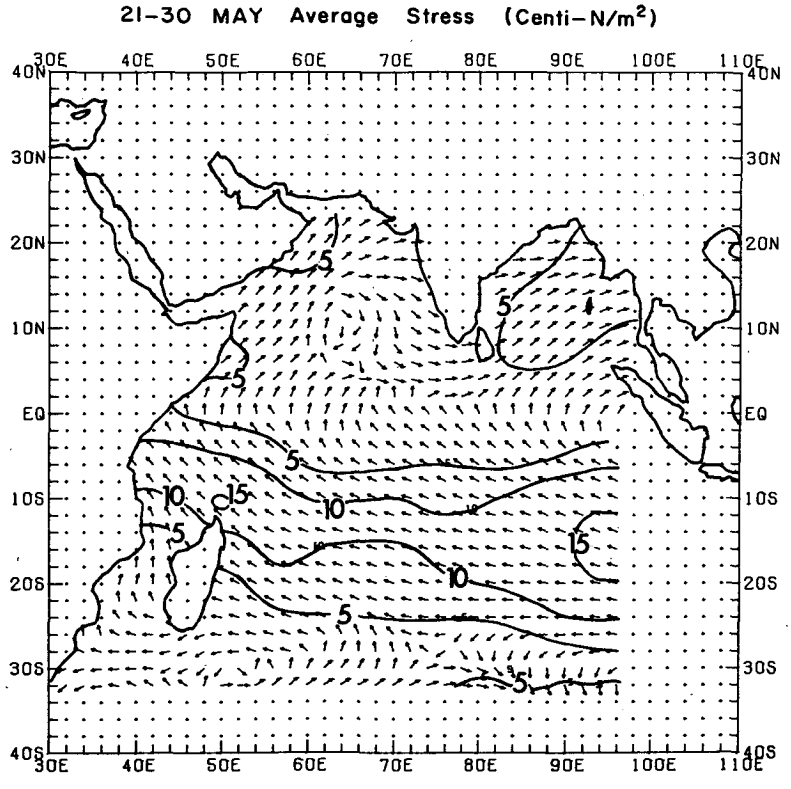

FIG. 6. Wind stress from 21 to 30 May 1979.

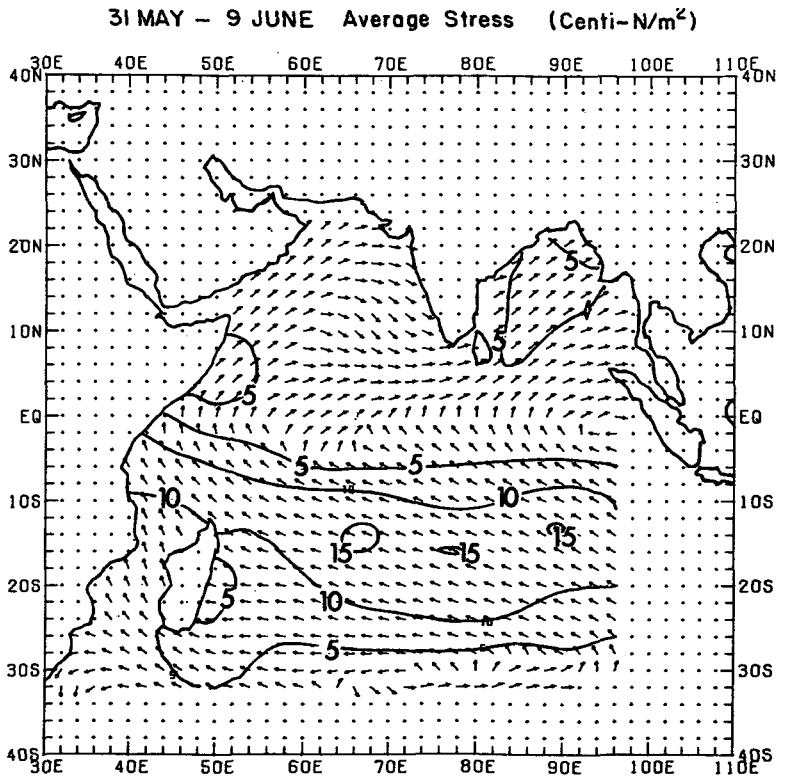

FIG. 7. Wind stress from 31 May to 9 June 1979.

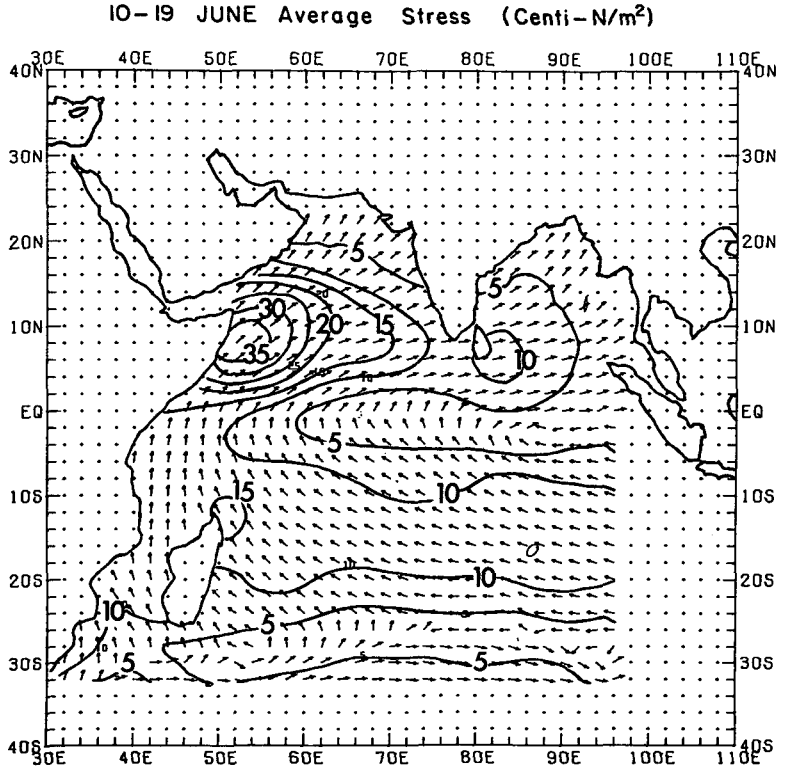

FIG. 8. Wind stress from 10 to 19 June 1979.

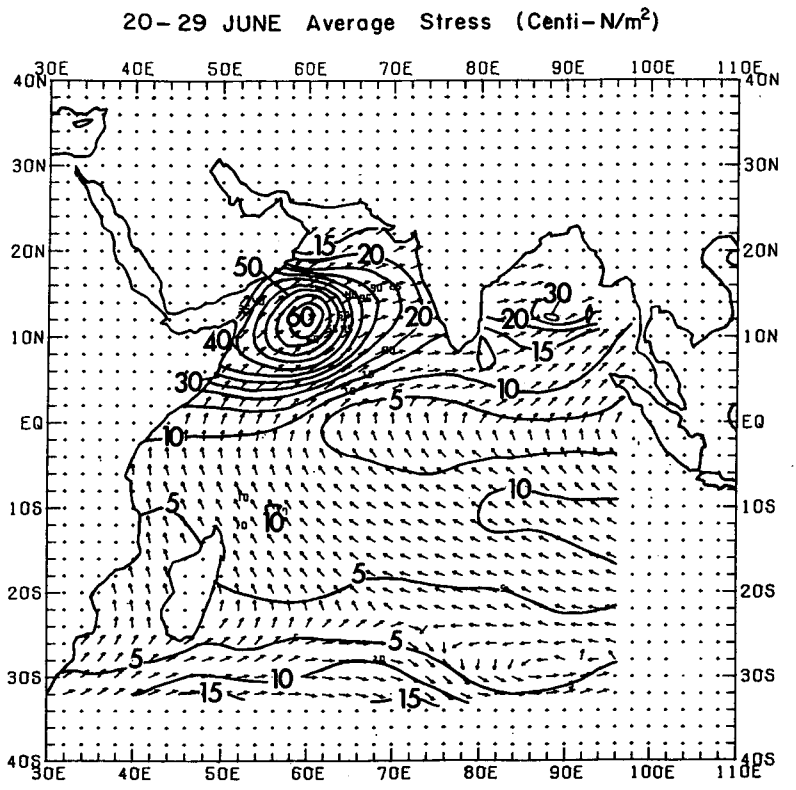

FIG. 9. Wind stress from 20 to 29 June 1979.

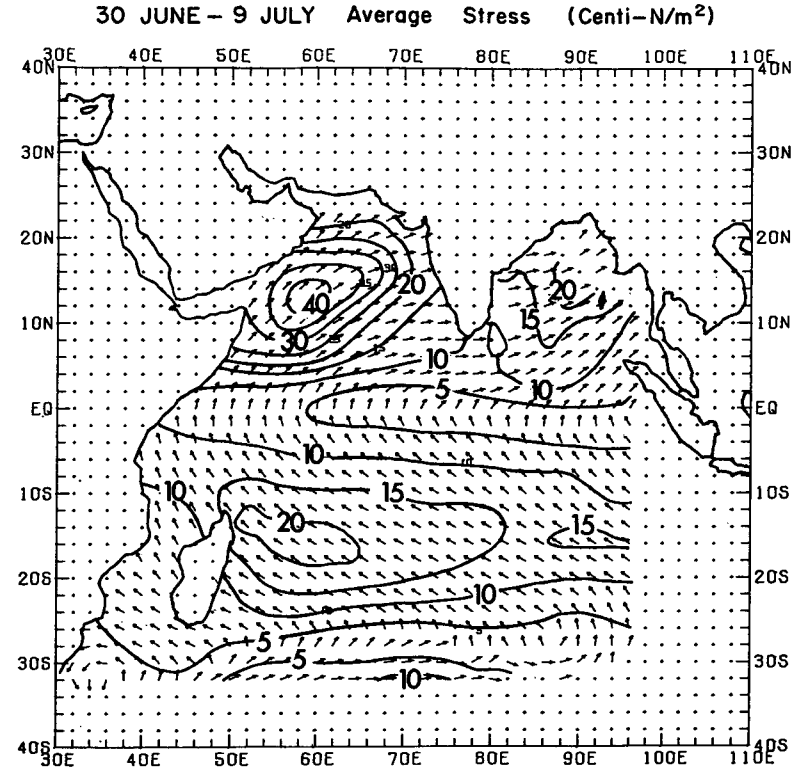

FIG. 10. Wind stress from 30 June to 9 July 1979.

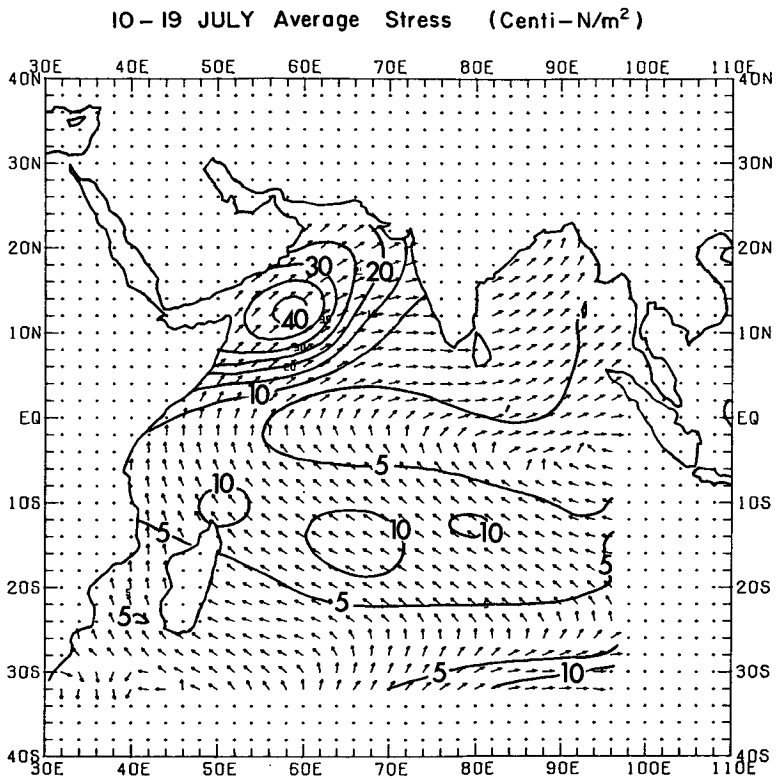

FIG. 11. Wind stress from 10 to 19 July 1979.

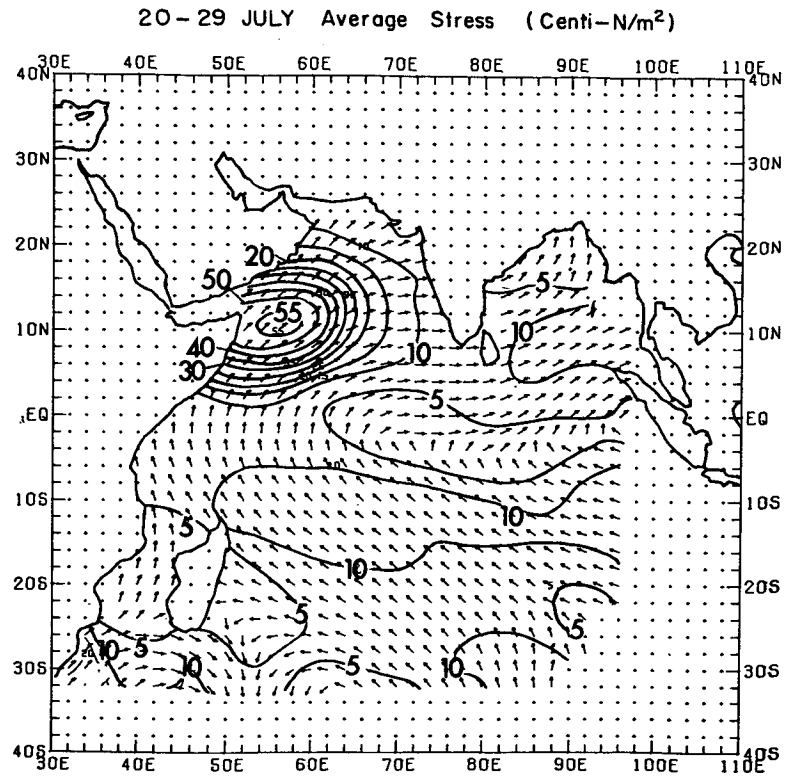

FIG. 12. Wind stress from 20 to 29 July 1979.

by a large sample of low-level clouds and the Arabian Sea was adequately covered by the merchant ship reports.

In the second 10-day period (11–20 May, Fig. 5) the trade winds remained strong on the eastern side of the ocean along a line from 80 to 90°E, at 18°S. This area was south of the southern vortex and thus it probably was enhanced by the vortex. In the Bay of Bengal a stronger southwesterly flow appeared from 11 to 20 May. Prior to this time the flow seemed unorganized in this area.

From 21 to 30 May (Fig. 6) the trade winds diminished in strength compared to the previous 10 days. The vortex in the Southern Hemisphere was no longer found on the daily analyses. Along the equator east of 65°E southerly and southeasterly winds were found where previously southwesterly winds were present. In the Arabian Sea a weak anticyclonic vortex continued while in the Bay of Bengal the southwesterly winds diminished in strength.

From 31 May to 9 June (Fig. 7) the stress pattern was similar to the preceding periods. The trade winds appeared to increase slightly over the previous 10-day period.

The strong southwesterly winds of the Somali Jet first appeared on 12 June (Fig. 8). The 10–19 June period depicted the full monsoon pattern with a very strong jet east of Africa at 8°N and 52°E, with stress >0.35 N m^{-2}. The southwesterly winds in the Bay of Bengal also appeared to increase in strength. South of the equator, the trades remained at nearly the same strength.

The period from 20 to 29 June (Fig. 9) exhibited the highest wind stress in the Somali Jet, 0.6 N m^{-2} at 12°N and 60°E. The center of the jet moved northeast (downwind) from its position in the previous period. The entire Arabian Sea was dominated by strong southwesterly winds. The southwesterly winds in the Bay of Bengal peaked in strength during this period exerting a maximum stress of 0.3 N m^{-2}. In contrast to the high winds in the Northern Hemisphere, the Southern Hemisphere trades weakened in intensity.

From 30 June to 9 July (Fig. 10) the trades increased in strength while the winds in the northern Hemisphere decreased in strength. During the period of strong trade winds, the highest stress values were found to the east of Madagascar. In all the previous

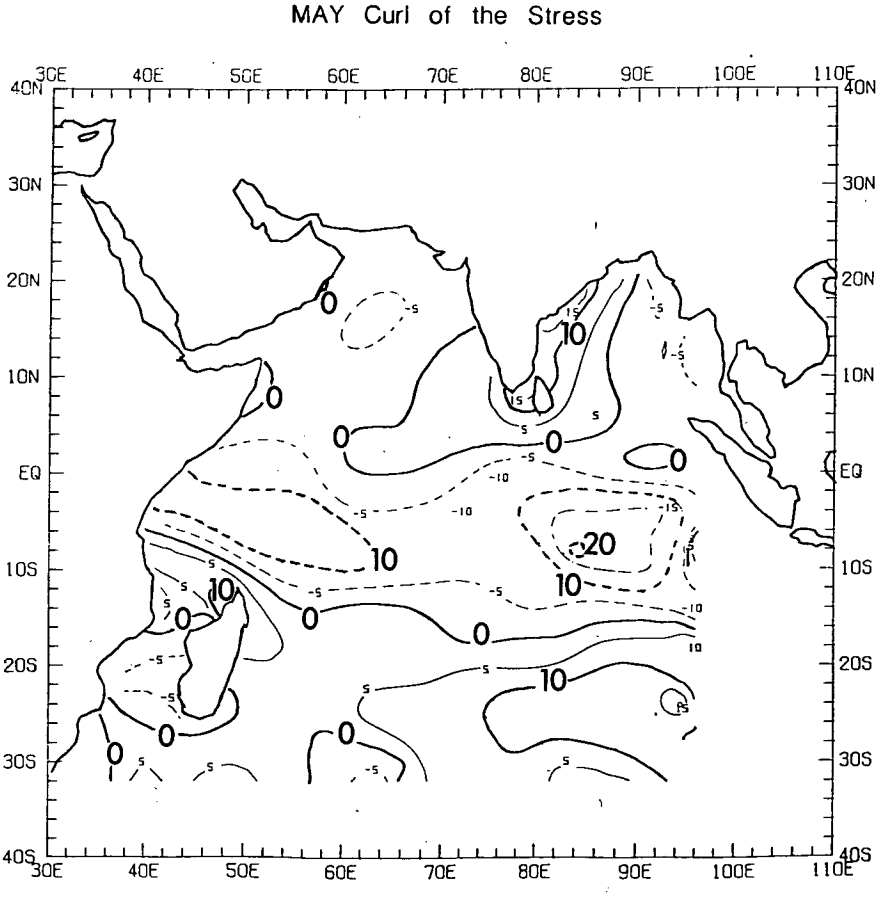

FIG. 13. Average vertical compment of $\nabla \times \tau$ for the month of May 1979 calculated from 2° latitude × 2° longitude grids on a daily basis. Units are 10^{-8} N m^{-3}. Anticyclonic values (negative) are shown dashed.

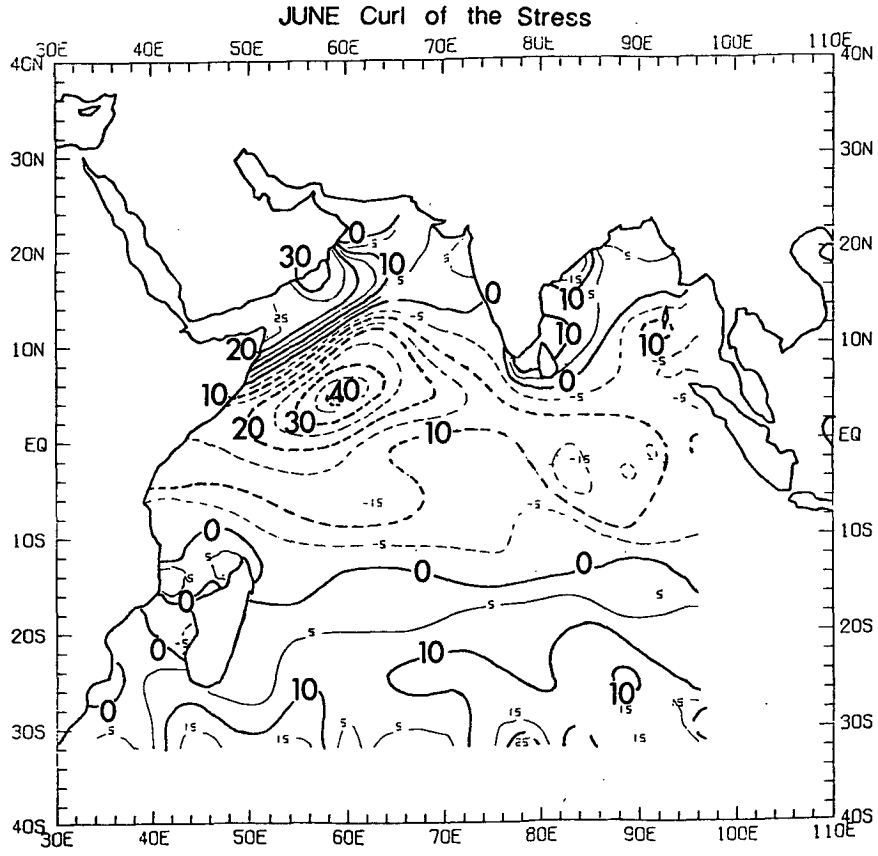

FIG. 14. Average vertical compment of $\nabla \times \tau$ for June 1979. Units are 10^{-8} N m^{-3}. Negative values are shown by dashed curves.

analyses the trade winds peaked in two locations: north of Madagascar, and on the eastern side of the Indian Ocean. This period exhibied a change in the pattern of the trades with the strongest winds on the western side of the ocean.

From 10 to 19 July (Fig. 11) the trades weakened in strength. However, the largest change was in the Bay of Bengal where the southwesterly winds dropped to the levels that existed before the monsoon developed. The Somali Jet exhibited only a slight decrease in strength during the period.

From 20 to 29 July (Fig. 12) the Somali Jet increased in strength and its center shifted slightly to the southwest (upwind) by 2° of latitude and longitude to 10°N, 56°E. Also of importance was the extension of the westerly winds in the Northern Hemisphere across the equator in the center of the ocean from 70°E to 80°E. The east–west line that separated the easterly trades from the westerlies appeared to migrate south during this time. The trades south of the equator increased in strength from 20 to 29 July despite the shift of the westerlies.

6. Curl of the stress

The vertical component of the curl of the stress is an important parameter. (For simplicity in the discussion below we take "curl" or "curl of the stress" to refer to the vertical component only). The curl constitutes the forcing for Sverdrup transport in steady ocean circulations. For large ocean basins steady conditions of Sverdrup transport are achieved on a time scale or the order of years. However, variations of the curl on shorter time-scales will excite transient or wave-like displacements of the density stratification which may be raised or lowered by Ekman pumping.

We evaluated the curl on a daily analysis. Monthly averages are presented here. These were obtained by averaging the daily analyses and are intended to enhance our understanding of seasonal changes of the pycnocline.

a. May 1979

During May the curl was strongest in the area of the vortex that was found in the Southern Hemisphere as previously discussed (see Fig. 13 at 6°S, 88°E). A persistent band of negative curl extended across the whole study region in the Southern Hemisphere from the equator to 12°S. This was a reflection of the turning of the trade winds toward the north shown in Fig. 1. Around the eastern coast of India a strong positive curl was found resulting from

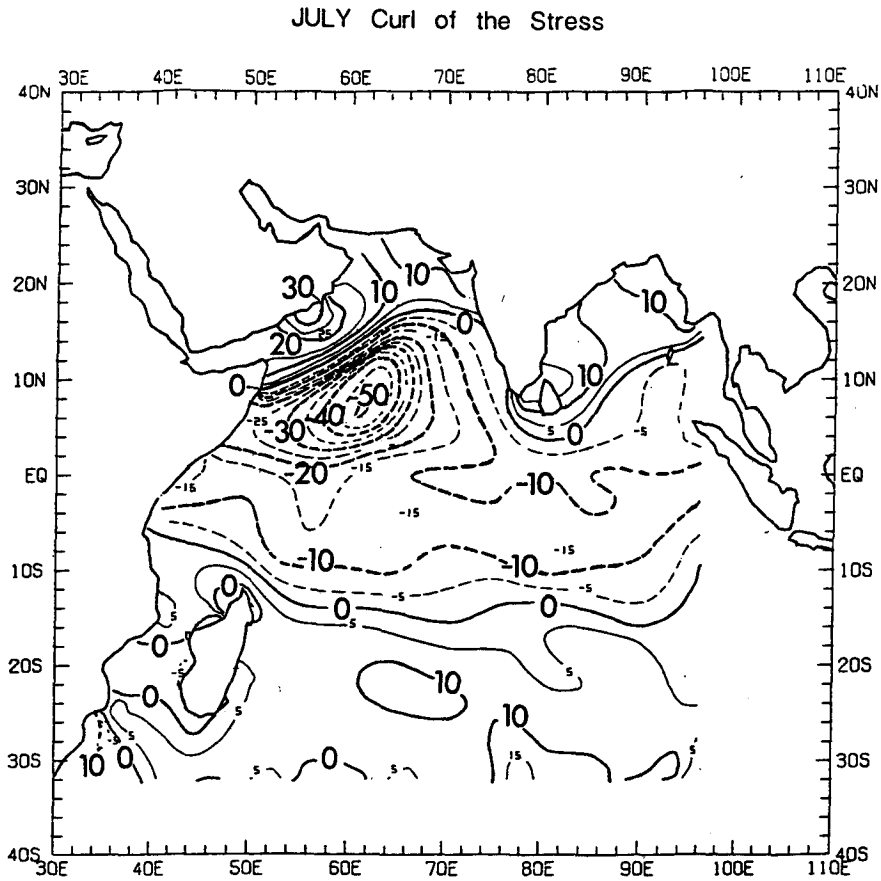

FIG. 15. Average vertical compment of $\nabla \times \tau$ for July 1979. Units are 10^{-8} N m^{-3}. Negative values are dashed.

the southwesterly winds in the Bay of Bengal which were strongest near the center of the Bay. In the Arabian Sea the curl was extremely small because of the light wind conditions that existed there during the entire month.

b. June 1979

During June the dominant feature was the Somali Jet as shown in Fig. 2. The curl exhibited strong anticyclonic values (−) to the southeast and strong cyclonic values (+) to the northwest (Fig. 14). The contours between these extremes depicted the axis of the Jet. An area of strong (−) curl was found at 3°S, 82°E where the easterly trades turned toward the north. The belt of turning winds (to the north) in general exhibited moderate values over most of the area between the equator and 12°S. An important increase in (+) curl along the eastern coast of India resulted from the strengthening of the winds in the Bay of Bengal.

c. July 1979

In July (see Fig. 15) the (−) curl southeast of the Somali Jet was even stronger than in June. On both sides of this jet the gradient in wind speeds was larger than in the previous month. The latitudinal belt where the trades turned north exhibited a near-uniform curl across the whole ocean with no obvious maxima. The (+) curl on the eastern coast of India decreased reflecting the weakening of the winds in the Bay of Bengal during the month.

It is interesting to compare our July curl field with the July chart of Hastenrath and Lamb. Both show a general pattern of moderate (+) values south of 15°S in the zone from 45E to 100°E, (+) values north of 15°N and a prominent (−) feature at 6°N, 60°E. A closer comparison reveals differences. For example, there are features in the climatological chart which are subdued in the 1979 data. Among these are both minima (near 5°S, 70°E, 12°S, 78°E; 8°N, 92°E) and maxima (near 7°N, 83°E; 22°N, 68°E; 15°N, 56°E). Some of the above differences occur in areas of poor coverage in the climatological data [e.g., ~100 observations per grid point for all months in the 60 years from 1911 to 1970, as shown by Chart No. 1 of Hastenrath and Lamb (1979)]. Consequently, alias effects as well as the peculiarities of a particular year may explain these differences.

7. Summary and discussion

By comparing our analyses for the monsoon of 1979 with the Hastenrath and Lamb (1979) climatology, areas where major differences from the long-term mean became apparent. The most notable differences were found in May. The Somali Jet was completely absent during May of 1979. This deviated from more typical years for which the onset of the monsoon is earlier. A second major deviation from the climatology was the strength of the trades in the eastern Indian Ocean during May and the strong westerly Jet that occurred on the equator in the early part of the month. As one would expect, the strong vortex we found in the Southern Hemisphere was not as evident in the climatological average.

The strengthening of the Southern Hemisphere trades that occurred when the Somali jet decreased slightly from 30 June to 9 July (Fig. 10) was also worth noting. Later, when the jet was at its strongest intensity (from 20–29 July as shown in Fig. 12), the trades had weakened slightly. This suggests a possible phase oscillation between the two hemispheres.

The extremely high stress values exerted by the Somali Jet are remarkable in themselves. Because the cubic relationship between wind speed and surface stress becomes dominant for speeds above 10 or 12 m s^{-1}, the jet exerted over three times the stress of the Southern Hemisphere trades.

Acknowledgments. The authors are grateful to the FGGE wind trackers at Wisconsin for their conscientious efforts in transforming satellite imagery into meaningful wind analyses. Without their efforts the stress analyses would have been more difficult. We also appreciate the help of Cecil Lo and Hassan Virgi in developing the gridding techniques. This research was funded by NSF grant ATM79-13097.

REFERENCES

Bruce, J. G., 1978: Spatial and temporal variation of the wind stress off the Somali Coast. *J. Geophys. Res.*, **83,** 963–967.

Endlich, R., and R. Mancuso, 1968: Objective analysis of environmental conditions associated with thunderstorms and tornadoes. *Mon. Wea. Rev.*, **96,** 342–350.

Fein, J. S., and J. . Kuettner, 1980: Report on the summer MONEX field phase. *Bull. Amer. Meteor. Soc.*, **5,** 461–477.

Hastenrath, S., and P. J. Lamb, 1979: *Climatic Atlas of the Indian Ocean, Part I: Surface Climate and Atmosphere Circulation.* University of Wisconsin Press, 97 pp.

Hellerman, S., 1967: An updated estimate of the wind stress on the world ocean. *Mon. Wea. Rev.*, **95,** 607–620.

Mosher, F. R., 1979: Cloud drift winds from geostationary satellites. *Atmos. Techn.*, NCAR, No. 10, 53–60.

Rao, P. K., 1980: The tropical disturbances over the Indian Ocean. *Mon. Wea. Rev.*, **108,** 1054–1055.

Wu, J. 1980: Wind-stress coefficients over sea surface near neutral conditions—a revisit., *J. Phys. Oceanogr.*, **10,** 727–740.

Wylie, D. P., and B. B. Hinton, 1981: The feasibility of estimating large-scale surface wind fields for the summer MONEX using cloud motion and ship data. *Boundary-Layer Meteor.*, **21,** 357–367.

Young, J. A., H. Virgi, D. P. Wylie and C. Lo, 1980: Summer monsoon windsets from geostationary satellite data. Space Science and Engineering Center, University of Wisconsin, 127 pp.